Proceedings of the 21st ICSMGE, Vienna, Austria, 14 – 19 June 2026. Pistrol, Adam & Schweiger (eds.)
Published by: ÖGG, Austrian Society for Geomechanics, Salzburg, Austria, ISBN 978-3-9503898-4-5
https://doi.org/10.53243/ICSMGE2026-1751

Numerical analysis of helical pile foundations for offshore wind turbines

Alkmini-Chara Livanidou, Konstantinos Georgiadis, Yannis K. Chaloulos
Department of Civil Engineering, Aristotle University of Thessaloniki, Greece, alkminili@civil.auth.gr

David M. G. Taborda
Department of Civil and Environmental Engineering, Imperial College London, United Kingdom

ABSTRACT: Many countries, including the EU member states and the US, have legislated a transition from traditional fuels to renewable energy sources, with offshore wind power expected to play a key role in this shift. Given that foundation type accounts for approximately 30% of the total cost, their selection and installation are crucial decisions. Monopiles are currently the most commonly used foundation type, representing about 80% of existing Offshore Wind Turbines (OWT) foundations. However, installing them significantly disturbs the seabed and presents difficulties in deeper waters, increasing interest in alternative foundation solutions. This study examines helical piles as a more economical and lower-footprint option compared to conventional piles. Their response in sand under monotonic lateral loading is investigated through advanced three-dimensional numerical analyses employing state-of-the-art constitutive models and special interface elements. A bespoke script extracts p-y curves from the three-dimensional analysis. A series of parametric analyses were performed to examine the influence of the number and location of helices and to develop design recommendations for optimized OWT foundations. The analyses consider three relative densities (D_r) of Dunkirk sand.

KEYWORDS: Offshore wind turbines, anchors, deep foundations, helical piles, numerical analysis.

1 INTRODUCTION

In recent years, offshore wind energy has gained significant attention as a key component of the transition toward sustainable energy systems. The most common type of foundation for Offshore Wind Turbines (OWTs) is currently the monopile foundation (Gupta & Basu 2020). Fixed-bottom foundations, such as monopiles, are cost-effective for water depths up to 60 meters; beyond this depth, the use of floating foundation concepts is being increasingly explored.

Helical piles have also been proposed as a viable foundation option for OWTs. This concept was initially proposed by Byrne & Houlsby (2015). Helical piles have been primarily used as a foundation solution for onshore structures in several countries, such as the United States (Perko 2009; Spagnoli & Tsuha 2020). Currently, they are extensively employed to support transmission towers and pipelines due to their ability to resist pull-out loads and serve as countermeasures against liquefaction (Orang et al. 2021).

Helical piles have several advantages. First, for the same volume of steel, they provide significantly greater uplift capacity than conventional piles due to their unique geometry. This improvement in performance can be achieved with minimal additional cost, as the circular plates constitute only a small portion of the total construction material. Additionally, they exhibit excellent seismic performance (Elsawy et al. 2019). Typically, installation is carried out through screwing, which results in reduced environmental impact. Moreover, their potential for reuse has led to their classification as a green foundation system (Ullah et al. 2019). Finally, they are adaptable to diverse foundation configurations, making them suitable for varying water depths and complex loading conditions.

Among the key design challenges for OWTs are the lateral forces generated by wind and ocean currents. Given the unpredictable nature of the offshore environment, understanding their lateral response is particularly important. Moreover, the need to address this issue is amplified by ongoing efforts to expand the offshore wind turbine industry into deeper waters and stronger wind currents, where such design challenges are expected to become increasingly significant.

The aim of this paper is to examine the behaviour of helical piles in sand under monotonic lateral loading. Through advanced three-dimensional numerical analyses, the parameters influencing the p-y response are investigated. It is important to highlight that, this study models the actual geometry of the helices, unlike conventional approaches where helices are idealized as flat plates. Hence, the effect of helix shape can be investigated as also explored in previous work by Stefopoulos et al. (2023).

2 FINITE ELEMENT ANALYSES

All analyses were conducted using the finite element software PLAXIS 3D (Version 2024.2.0.1144, Bentley Systems, 2024). In all cases, the numerical model simulates a single helical pile in sand subjected to lateral loading under drained conditions. Helical piles with one or two helices are considered. The primary objective of the simulations was to investigate the influence of the number of helices and sand density on the horizontal capacity and load transfer mechanisms of the pile.

2.1 *Soil modelling*

The constitutive model selected to simulate the mechanical behavior of the sand is the IC-MAGE M02 model, developed by Taborda et al. (2022). It is implemented in PLAXIS 3D as a User-Defined Soil Model (UDSM) as described in Taborda et al. (2024). The model uses the concept of the state-parameter ψ, which has been extensively described in the literature (Been & Jefferies 1985; Jefferies & Been 2006). It extends the Mohr-Coulomb failure criterion by introducing a non-associated flow rule and by using the state-parameter ψ in its formulation, ensuring the model captures key aspects of soil behavior under monotonic loading. Hence, both the shearing resistance angle φ_c, which governs the available strength, and the dilatancy angle ν_c, which controls the plastic behaviour, are influenced by the state-parameter ψ.

Three different initial relative densities of Dunkirk sand were investigated D_r = 40%, 60% and 80%. A previously established model calibration for Dunkirk sand, as employed in the study by Tantivangphaisal et al. (in press), was adopted in the present paper. All model parameters used in the simulations are summarized in Table 1.

Table 1. Parameters for calibrated Dunkirk sand.

Parameter	Value	Unit
G_{ref}	94.4	MPa
v	0.18	-
p'_{ref}	101.3	kPa
m_G	0.515	-
a	$9.25 \cdot 10^{-3}$	%
b	0.765	-
R_{min}	0.104	-
$e_{cs,ref}$	0.910	-
λ	0.135	-
ξ	0.179	-
φ'_{cs}	33.9	°
k	2.34	-
l	3.91	-

2.2 *Geometry*

The pile shaft was modelled as a hollow steel cylinder with an outer diameter D_p = 0.40 m and wall thickness t = 0.01 m. The total length of each pile was L = 8.0 m. The helices had a diameter of D_h = 1.60 m and a pitch of p = 0.40 m. For the double-helix configuration, the vertical spacing between the helices was equal to half the helix diameter (d = 0.80 m). The first helix was placed 0.80 m below the pile head, z_{h1} = 0.80 m, while the second was located at a depth of z_{h2} = 1.60 m. Both the shaft and the helices were modelled as elastic with the properties of steel i.e., Young's modulus E = 210 GPa and Poisson's ratio v = 0.2. The helical pile was 'wished-in-place'.

Interface elements were used to simulate the interaction between the soil and structural components. In the numerical model, these elements adopted a Mohr-Coulomb failure criterion and were defined using a direct stiffness approach. Both normal and shear stiffness values were set equal to $k_n = k_s = 10^5$ kN/m³, ensuring a sufficiently rigid interface. The interface friction angle was taken equal to that of the adjacent soil at Critical State (ϕ_{inter} = 33.9°), while the dilation angle and the cohesion were set to zero (ψ_{inter} = 0°, c_{inter} = 0.0).

The model dimensions were 20 m × 12 m × 8 m (width × depth × height), corresponding to 50D × 30D × 20D, relative to the pile diameter. A typical geometry representation of the numerical analysis is shown in Figure 1. These dimensions were selected to ensure full development of the failure mechanism. To accurately capture the pile behavior under lateral loading, the finite element mesh consisted of approximately 30,000 to 45,000 elements.

Different zones of mesh refinement were introduced. Two cylindrical regions were defined around the pile. The first extends along the entire pile shaft and the second surrounds the helix zone. The soil was modelled using 10-node tetrahedral elements, while the shaft and helices were modelled with 6-node plate elements. Along the shaft-soil and helix-soil interfaces, 12-node interface elements were placed to allow for relative displacement and realistic load transfer.

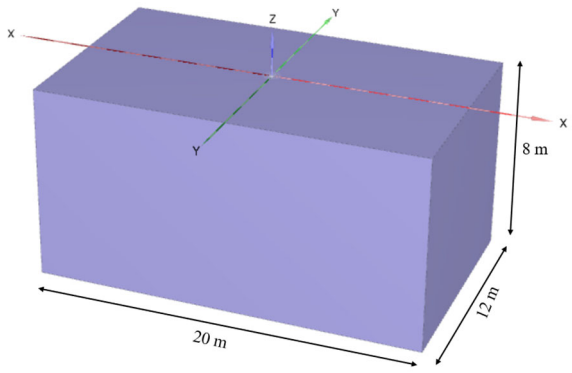

Figure 1. Geometry of numerical model.

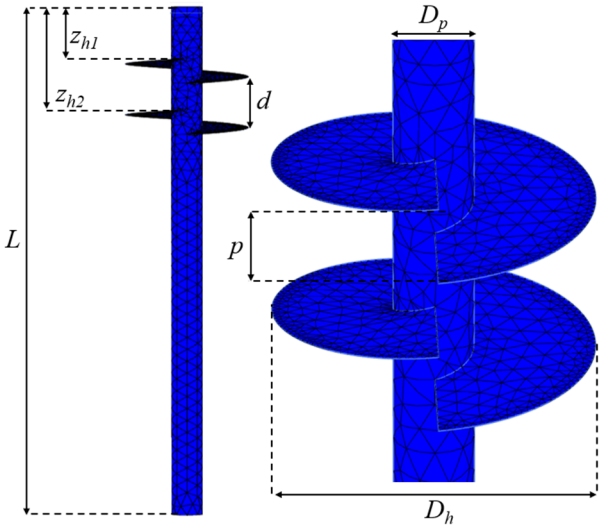

Figure 2. Typical representation of the double-helix pile: (Left) overall geometry of pile; (Right) detailed view of the mesh distribution on the helices and the shaft.

The vertical boundaries of the mesh were constrained in the normal direction and the bottom boundary was fully fixed. Horizontal displacements were applied at the pile head through a specially designed rigid loading plate, ensuring uniform deformation. The imposed displacement was increased incrementally until failure was observed, here assumed to correspond to a mudline displacement of $u_x = D_p$ = 0.40 m.

As previously mentioned, unlike traditional approaches, this study explicitly models the helices in their full three-dimensional shape, allowing for a more accurate representation of their behavior. An image of a typical configuration of a double-helix pile is shown in Figure 2.

3 RESULTS AND DISCUSSION

A series of displacement finite element analyses was conducted to examine the influence of the presence and number of helices close to the ground surface on lateral pile behaviour, for sands with different relative densities (D_r). To evaluate the effect of helix configuration on lateral pile response, the results are presented in the form of load–displacement diagrams (F_x–u_x, Figure 3), percentage of force increase (Table 2) and p-y curves (Figure 4).

Figure 3 illustrates the lateral load response for piles with and without helices, for three relative densities of Dunkirk sand i.e., D_r = 40%, 60%, and 80% (blue, red and green lines respectively). Each configuration was analyzed for a shaft-only pile (SO, continuous lines), a single helix (SH) placed at two different depths i.e., z_h = 0.80 and 1.60 m (chain and dashed lines), and a double-helix configuration (DH, dotted lines).

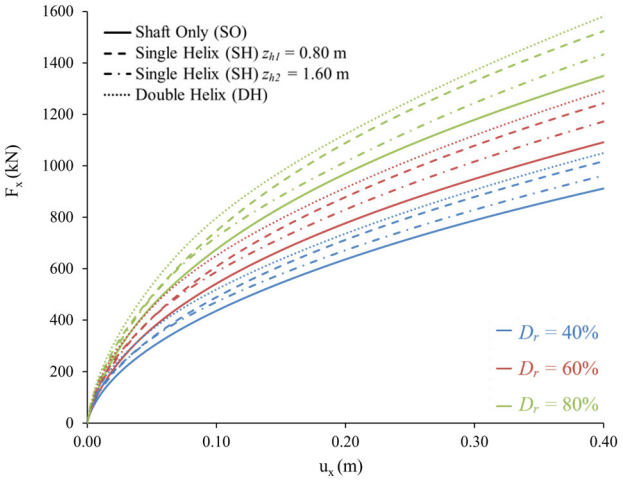

Figure 3. Load-displacement curves for each pile configuration.

Table 2. Lateral resistance and corresponding percentage increases for each pile configuration.

D_r	Pile type	ΔF_x (%) at u_x/D_p = 0.01, 0.1 and 1		
		0.01	0.1	1
40%	Single Helix z_{h1} = 0.80m	35.2	11.4	11.7
	Single Helix z_{h2} = 1.60m	12.7	10.7	5.5
	Double Helix	38.5	22.4	15.1
60%	Single Helix z_{h1} = 0.80m	28.6	12.1	13.9
	Single Helix z_{h2} = 1.60m	13.5	10.6	7.5
	Double Helix	47.5	22.5	18.1
80%	Single Helix z_{h1} = 0.80m	29.8	9.2	12.6
	Single Helix z_{h2} = 1.60m	6.6	8.1	5.9
	Double Helix	41.2	18.8	16.9

To quantify the effect of increasing the helix depth and the number of helices, the percentage increase in lateral resistance (ΔF_x) was calculated with reference to the shaft-only configuration. The calculations for all cases are presented in Table 2.

The lateral load–displacement curves presented in Figure 3, along with the corresponding values summarized in Table 2, clearly demonstrate the beneficial effect of helical plates on the lateral resistance of piles in sand. For all examined relative densities (D_r) the addition of one or two helices results in a substantially enhanced lateral response compared to the shaft-only configuration.

The increase in lateral resistance is particularly notable at small displacements ($u_x = 0.01 \cdot D_p$). For example, in loose sand (D_r = 40%) the double-helix configuration resulted in a 38.5% increase in lateral force, while in dense sand (D_r = 80%) the improvement reached 41.2%. These findings highlight the effectiveness of helices in the early stages of lateral loading.

However, this beneficial effect diminishes as displacement increases. At $u_x = D_p$, the corresponding percentage increase drops significantly (e.g., 15.1% for D_r = 40%, and 16.9% for D_r = 80%), suggesting that the contribution of helices becomes smaller. Despite the reduction, the improvement of approximately 15% in some cases may still be considered an important contribution to pile performance under large lateral displacements.

The depth of the helix also plays a significant role in the pile's performance. In all cases, the shallow-helix configuration (z_{h1} = 0.80 m) provides higher lateral resistance than the deeper one (z_{h2} = 1.60 m), particularly at low and medium displacement levels. For instance, in dense sand (D_r = 80%) the shallow-helix configuration the increase in the resistance relative to the deeper-helix configuration at small displacements is approximately five times larger. At medium displacement levels, the difference becomes less pronounced, approaching similar performance. However, at $u_x = D_p$, the shallow helix still outperforms the deeper one, with nearly twice the percentage increase.

In addition, lateral soil reaction (p–y curves) were extracted at multiple depths along the pile shaft. Figure 4 presents the p-y curves at depths z = 1.0, 2.0, 3.0 and 4.0 meters for different values of relative density (D_r = 40%, 60% and 80%) and helix configurations (shaft-only, single-helix at z_{h1} = 0.80 m, single- helix at z_{h2} = 1.60 m). These curves allow the examination of how the presence and position of helices influences the lateral soil resistance on the pile shaft.

The obtained curves were generated using a bespoke Python script specifically developed for this purpose. The data were extracted from the 3D numerical model, ensuring consistency across all pile configurations and depths. The post-processing procedure involved retrieving the distributed soil reaction force p (in kN/m) acting on the pile surface at each depth, and plotting it against the corresponding local lateral displacement y (in m) of the pile.

Three zones can be identified with different helix effects on the lateral resistance on the shaft. In Zone 1, from the ground surface to the bottom of the helix (1.2 m for the shallow helix or 2 m for the deeper helix), the presence of the helix appears to moderately reduce the lateral resistance on the pile shaft, for all examined relative densities. This is evident in Figure 4a for the shallow helix (z_{h1} = 0.8 m) and in Figure 4a,b for the deeper helix. This behaviour indicates that, at these depths, a significant portion of the lateral resistance is applied on the helix directly and not on the shaft and that additional springs for the helix need to be introduced in a helical pile p-y analysis to capture this effect.

The opposite behaviour is observed below the bottom of the helix (Zone 2), below 1.2 m for the shallow helix case (Figure 4b,c) and below 2 m for the deeper helix case (Figure 4c), where a small to moderate increase in shaft resistance is observed for all relative densities. This increase in resistance below the helix combined with the observed decrease in Zone 1 that was discussed above, shows that the helix leads to a small to moderate redistribution of lateral resistance along the pile shaft. Clearly, this redistribution may need to be accounted for in p-y analyses.

Finally, at greater depths (Zone 3), there appears to be no effect of the helix on the lateral saft resistance, as illustrated in Figure 4d.

4 CONCLUSIONS

This study presents a numerical investigation on the lateral behavior of a pile with diameter 0.40 m embedded in Dunkirk sand at three relative densities (D_r = 40%, 60%, and 80%). Four pile configurations were analyzed: a shaft-only pile, single-helix piles with helices at depths of 0.80 m and 1.60 m, and a double-helix pile with helices at depths of 0.80 m and 1.60 m.

All helices had a diameter of 1.60 m. The performance of each configuration was evaluated by comparison against the shaft-only pile.

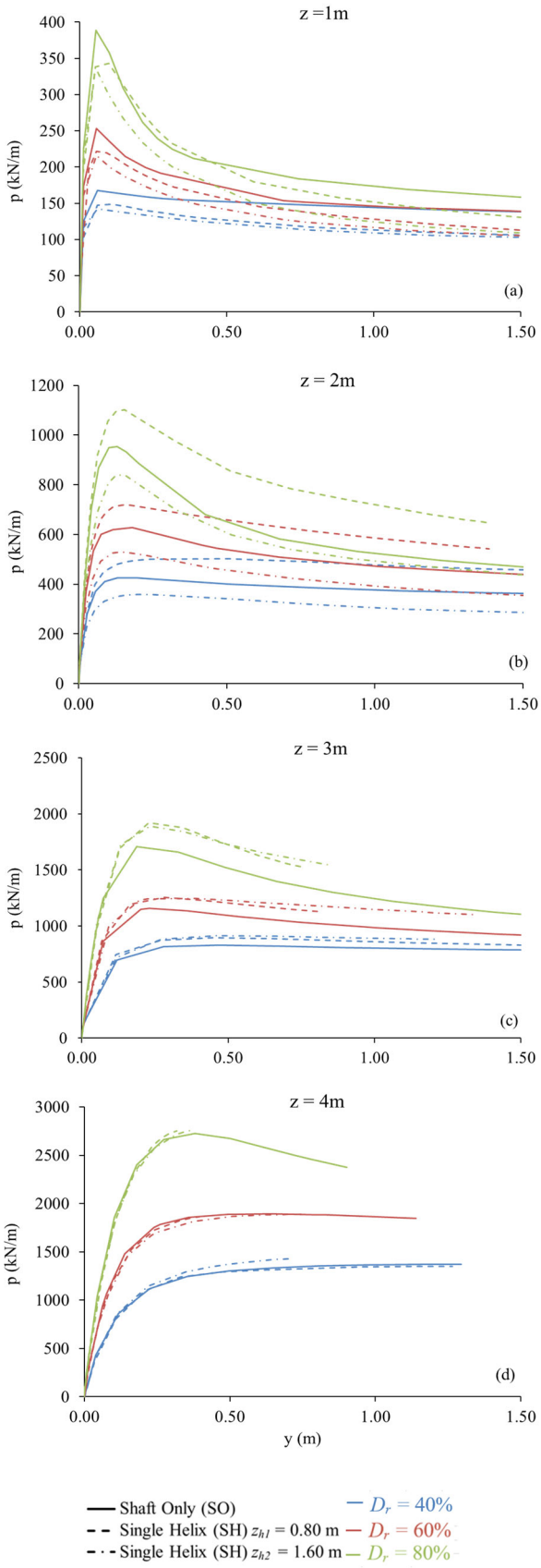

Figure 4. Lateral soil reaction curves (p–y curves) at different depths, from top to bottom: z = 1.0 m; z = 2.0 m; z = 3.0 m and z = 4.0 m.

For all cases examined, the beneficial contribution of the helix is significant during the early stages of lateral loading. As the loading increases, this benefit gradually reduces; however, it remains substantial, particularly for the shallow-helix configuration and the double-helix arrangement. In all cases, the double-helix configuration outperforms single helical piles. Helix embedment depth was found to be a critical parameter as a shallow helix has better lateral response than the deeper helix.

Analysis of p-y curves extracted from the numerical results, revealed that the effect of the helix on the lateral soil resistance on the pile shaft is to decrease lateral resistance above the helix, while increasing it in a limited zone immediately below the helix. No effect was observed at greater depths. These observations were made for all sand relative densities considered. In all cases investigated, it is apparent that considering only the local lateral soil reactions would lead to an underestimation of the load-displacement behaviour of helical piles, indicating that, in order to use p-y methods for this type of foundations, new springs need to be introduced to take into account the contribution of the helix.

5 REFERENCES

Been, K. and Jefferies, M.G. 1985. A state parameter for sands. *Geotechnique* 35(2), 99–112.

Bentley Systems, 2024. *PLAXIS 3D 2024.1: 2 – Reference Manual.*

Byrne, B.W. and Houlsby, G.T. 2015. Helical piles: an innovative foundation design option for offshore wind turbine foundations. *Philosophical Transactions A* 373.

Elsawy, M.K., El Naggar, M.H., Cerato, A. and Elgamal, A., 2019. Seismic performance of helical piles in dry sand from large-scale shaking table tests. *Geotechnique* 69(12), 1071–1085.

Gupta, B.K. and Basu, D. 2020. Offshore wind turbine monopile foundations: Design perspectives. *Ocean Engineering* 213, 107514.

Jefferies, M.G. and Been, K. 2006. *Soil Liquefaction: a critical state approach*. London: Taylor & Francis.

Orang, M. J., Boushehri, R., Motamed, R., Prabhakaran, A., Elgamal, A. 2021. An experimental evaluation of helical piles as a liquefaction-induced building settlement mitigation measure. *Soil Dynamics & Earthquake Engineering*, 151.

Perko, H.A. 2009. *Helical piles: a practical guide to design and installation*. Hoboken, NJ: John Wiley & Sons, Inc.

Spagnoli, G. and de Hollanda Cavalcanti Tsuha, C. 2020. A review on the behavior of helical piles as a potential offshore foundation system. *Marine Georesources & Geotechnology* 38(9), 1013–1036.

Stefopoulos, N., Georgiadis, K. and Nikolaidis, T. 2023. Undrained uplift capacity of single helical piles and helical pile groups. *Proc. 10th European Conference on Numerical Methods in Geotechnical Engineering (NUMGE 2023)*, London.

Taborda, D.M.G., Pedro, A.M.G. and Pirrone, A.I. 2022. A state parameter-dependent constitutive model for sands based on the Mohr-Coulomb failure criterion. *Computers and Geotechnics* 148, 104811.

Taborda, D.M.G., Pedro, A.M.G., Kontoe, S., Tsiampousi, A. 2024. IC MAGE Model 02 – Simple state parameter dependent model with isotropic nonlinear stiffness (Version 2.8). Zenodo. doi: 10.5281/zenodo.13917305.

Tantivangphaisal, P., Taborda, D. M.G, Kontoe, S., Liu, T. and Jardine, R. *in press*. Numerical modelling of the long-term cyclic response of laterally loaded piles driven in sands using the high-cycle accumulation framework. *Geotechnique.*

Ullah, S.N., Hu, Y. and O'Loughlin, C. 2019. A Green Foundation for Offshore Wind Energy – Helical Piles. *Proc. World Engineers Convention, WEC2019*, Melbourne, 272–285.